Contribution from the Department of Chemistry, Faculty of Science, Kyushu University, Hakozaki, Higashiku, Fukuoka 812, Japan

Noncovalent Interactions in Metal Complexes. 16.[1] Stereoselectivity of 1:3 Complexes of Sc, Y, La, Al, Ga, and In Ions with 4-(*l*-Menthyloxy)-1-phenyl-1,3-butanedione and 4-(*l*-Menthyloxy)-1-*p*-tolyl-1,3-butanedione

Hisashi Ōkawa,* Hirofumi Tokunaga, Tsutomu Katsuki, Masayuki Koikawa, and Sigeo Kida

Received March 3, 1988

1:3 complexes of Sc^{3+}, Y^{3+}, La^{3+}, Al^{3+}, Ga^{3+}, and In^{3+} with 4-(*l*-menthyloxy)-1-phenyl-1,3-butanedione (H(*l*-moba)) and 4-(*l*-menthyloxy)-1-*p*-tolyl-1,3-butanedione (H(*l*-moba-Me)) have been prepared, and their stereoselectivities have been examined in view of noncovalent interligand interactions. The distributions of the diastereomers for the relatively inert Al and Ga complexes are determined by ^1H NMR spectroscopy, and the results demonstrate that the *fac*/*mer* ((*fac*-Δ + *fac*-Λ)/(*mer*-Δ + *mer*-Λ)) ratio is larger than the statistical value (1/3) for all of the cases. On the basis of circular dichroism induced at the ligand π–π^* transition, the configuration of the preferred diastereomer in solution is determined as *fac*-Λ for all of the complexes. The stereoselectivity that produces the *fac*-Λ isomer is enhanced when the size of the central ion becomes larger. On the basis of these facts, the stereoselectivity of the complexes is attributed to the operation of a noncovalent interaction in the form of a left-handed three-bladed propeller, comprising three interligand *l*-menthyl/aryl contacts.

Introduction

Configurational control of metal complexes by means of noncovalent interligand interactions is of importance in view of the development of stereospecific reactions using such sterically controlled complexes. In the preceding papers of this series[1-12] we have shown that high stereoselectivity of metal complexes occurs if ligands used are designed so as to cause noncovalent interligand interactions when coordinated to a metal ion. In 1/3 complexes of chiral 1,3-diketones, 4-(*l*-menthyloxy)-1-phenyl-1,3-butanedione (H(*l*-moba)) (see Figure 1) and its homologues,[2-7] a significant stereoselectivity occurred to yield one of the diastereomers predominantly. Such a stereoselectivity was presumed to stem from the noncovalent interligand interaction operating between the *l*-menthyl and aryl residues as shown in Figure 2. It should be noted that such interligand interactions are highly effective for controlling the complex configuration of labile metal ions such as Mn^{3+} and Ln^{3+} (lanthanide ions),[2-6] though configuration control of labile metal complexes is otherwise difficult. Related studies on 1/3 metal complexes of (+)-3-(hydroxymethylene)camphor[12-14] and (+)-3-acetylcamphor[14-16] indicated a low stereoselectivity of the diastereomers, probably because of the absence of intramolecular interligand contact[17] in these complexes.

The depiction of the noncovalent interligand interaction in the form of a right-handed three-bladed propeller (Figure 2) was based on the configuration determined for the isolated species of the cobalt(III) and chromium(III) complexes but not on the real diastereomer distribution, because our attempts to resolve the diastereomers with the use of chromatography were unsuccessful owing to the extremely high solubility of the complexes in most organic solvents. For those inert complexes, however, we could not definitely rule out the possiblity that the *fac*-Δ form of the four diastereomers separated as crystals selectively. Further, the preferred configuration of the labile manganese(III) and lanthanide(III) complexes in solution has not definitely been determined.

In order to gain unambiguous evidence for the operation of the noncovalent interligand interaction to displace the equilibrium among the diastereomers, a more detailed investigation based on a series of metal complexes including labile and inert metal ions was needed. In this regard, stereoselectivities of the 1/3 complexes of IIIA (Sc, Y, La) and IIIB (Al, Ga, In) ions with H(*l*-moba) and 4-(*l*-menthyloxy)-4-*p*-tolyl-1,3-butanedione, H(*l*-moba-Me) (see Figure 1), have been investigated in our study. Of these metal ions Al^{3+} and Ga^{3+} are relatively inert, but the other ions are labile.[18,19] Hence, NMR spectroscopic investigations of the Al and Ga complexes enable us to determine the thermodynamic distributions of the diastereomers in solution. Further, these nontransition-metal complexes are expected to show circular dichroism (CD) induced at the π–π^* transition of the diketonate ion if there is any asymmetry or dissymmetry about the central ion.[20,21] Therefore, we can investigate the stereoselectivities of [M(*l*-moba)$_3$] and [M(*l*-moba-Me)$_3$] by means of CD and ^1H NMR spectroscopies. If the interaction shown in Figure 2 indeed operates in the complexes, the optimum contact between the *l*-menthyl and aryl groups must be dependent upon the size of the central ion. On this basis, we have inspected the noncovalent interligand interaction in terms of the ionic radius of the central metal, varying from 0.67 Å (Al^{3+}) to 1.20 Å (La^{3+}).

Experimental Section

Preparations. The ligands H(*l*-moba)[2] and H(*l*-moba-Me)[5] were prepared by the methods previously reported.

[Sc(*l*-moba)$_3$]. An aqueous solution of scandium nitrate was prepared by dissolving Sc_2O_3 (46 mg) in nitric acid (10%, 12 cm^3). To this solution was added a methanolic solution of H(*l*-moba) (480 mg). The pH of the solution was adjusted to 7.5 by adding LiOH·H_2O to give an oily substance, which was washed with water by decantation and crystallized from methanol as colorless microcrystals. The yield was 46%.

[Sc(*l*-moba-Me)$_3$]. This complex was obtained as colorless microcrystals in a preparation similar to that for [Sc(*l*-moba)$_3$].

[Y(*l*-moba)$_3$]. To an aqueous solution of yttrium nitrate, which was prepared by dissolving Y_2O_3 (56 mg) in nitric acid (10%, 15 cm^3), was added a methanolic solution of H(*l*-moba) (480 mg), and the mixture was neutralized by adding LiOH·H_2O with stirring to give a pale yellow mass. It was crystallized from an ethanol–methanol (1/1 in volume) mixture

(1) Part 15: Ōkawa, H.; Maeda, S.; Nakamura, M.; Kida, S. *Inorg. Chim. Acta* **1987**, *128*, 155.
(2) Okawa, H.; Ueda, K.; Kida, S. *Inorg. Chem.* **1982**, *21*, 1594.
(3) Nakamura, M.; Ōkawa, H.; Kida, S. *Inorg. Chim. Acta* **1984**, *96*, 111.
(4) Nakamura, M.; Ōkawa, H.; Kida, S.; Misumi, S. *Bull. Chem. Soc. Jpn.* **1984**, *57*, 3147.
(5) Nakamura, M.; Ōkawa, H.; Kida, S. *Bull. Chem. Soc. Jpn.* **1985**, *58*, 3377.
(6) Ōkawa, H.; Nakamura, M.; Shuin, Y.; Kida, S. *Bull. Chem. Soc. Jpn.* **1986**, *59*, 3657.
(7) Nakamura, M.; Ōkawa, H.; Itoh, T.; Kato, M.; Kida, S. *Bull. Chem. Soc. Jpn.* **1987**, *60*, 539.
(8) Nakamura, M.; Ōkawa, H.; Kida, S. *Chem. Lett.* **1981**, 547.
(9) Maeda, S.; Nakamura, M.; Ōkawa, H.; Kida, S. *Polyhedron* **1987**, *6*, 583.
(10) Nakamura, M.; Ōkawa, H.; Inazu, T.; Kida, S. *Bull. Chem. Soc. Jpn.* **1982**, *55*, 2400.
(11) Ōkawa, H.; Nakamura, M.; Kida, S. *Inorg. Chim. Acta* **1986**, *120*, 185.
(12) Lifschitz, I. *Recl. Trav. Chim. Pays-Bas* **1950**, *69*, 1495.
(13) Dunlop, J. H.; Gillard, R. D.; Ugo, R. *J. Chem. Soc. A* **1966**, 1540.
(14) Chen, Y. T.; Everett, G. N., Jr. *J. Am. Chem. Soc.* **1968**, *90*, 6660.
(15) King, R. M.; Everette, G. N., Jr. *Inorg. Chem.* **1971**, *10*, 1237.
(16) Springer, C. S., Jr.; Sievers, R. E.; Feibush, B. *Inorg. Chem.* **1971**, *10*, 1242.
(17) Horrocks, W. D., Jr.; Johnston, D. L.; MacInnes, D. *J. Am. Chem. Soc.* **1970**, *92*, 7620.
(18) Eigen, M. *Z. Elektrochem.* **1960**, *64*, 115. Eigen, M.; Tamon, K. *Ibid.* **1962**, *66*, 93, 107.
(19) Jackson, J. A.; Lemons, J. F.; Taube, H. *J. Chem. Phys.* **1960**, *32*, 553.
(20) Larsen, E.; Mason, S. F.; Searle, G. H. *Acta Chem. Scand.* **1966**, *20*, 191.
(21) Nagasawa, A.; Saito, K. *Bull. Chem. Soc. Jpn.* **1974**, *47*, 131.

0020-1669/88/1327-4373$01.50/0 © 1988 American Chemical Society

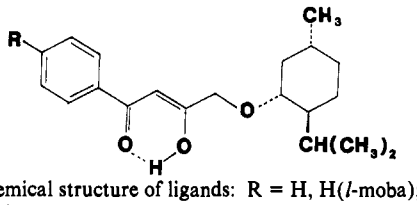

Figure 1. Chemical structure of ligands: R = H, H(*l*-moba); R = CH_3, H(*l*-moba-Me).

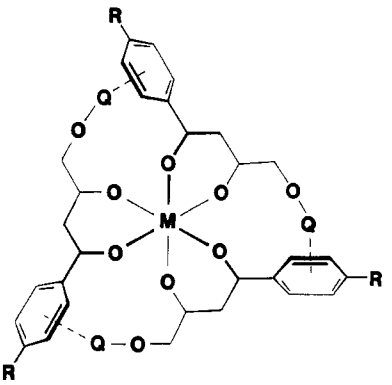

Figure 2. Schematic depiction of the noncovalent interligand interaction.

as almost colorless microcrystals. The yield was 57%.

[Y(*l*-moba-Me)$_3$]. This complex was obtained as colorless microcrystals in a preparation similar to that for [Y(*l*-moba)$_3$].

[La(*l*-moba)$_3$]. This complex was obtained by the reaction of lanthanum nitrate hexahydrate (220 mg) and H(*l*-moba) (470 mg) in a methanol–water mixture (7/3 in volume), using LiOH·H_2O as the neutralizing base. It was crystallized from ethanol as pale yellow crystals. The yield was 65%.

[La(*l*-moba-Me)$_3$]. This complex was obtained as pale yellow microcrystals in preparation similar to that for [La(*l*-moba)$_3$].

[Al(*l*-moba)$_3$]. A mixture of an ethanolic solution of H(*l*-moba) (0.5 g) and an aqueous solution of $Al_2(SO_4)_3$·$13H_2O$ (0.4 g) was neutralized with triethylamine and then heated at 80 °C for 2 h. The crude product, which was obtained on concentrating the solution, was dissolved in benzene, and the solution was subjected to an alumina column (10 mm × 100 mm). On evaporation of the solvent, [Al(*l*-moba)$_3$] was obtained as colorless microcrystals. The yield was 49%.

[Al(*l*-moba-Me)$_3$]. This complex was obtained and purified in a preparation similar to that for [Al(*l*-moba)$_3$].

[Ga(*l*-moba)$_3$]. To an ethanolic solution of H(*l*-moba) (0.6 g) was added dropwise an aqueous solution of $Ga_2(SO_4)_3$·$13H_2O$ (0.4 g). The mixture was made weakly alkaline with triethylamine (pH 7.5) and was stored overnight in a refrigerator. A white precipitate formed and was separated by filtration, washed with hot methanol to remove the free ligand involved as the impurity, and crystallized from ethanol. The yield was 67%.

[Ga(*l*-moba-Me)$_3$]. The synthesis for this complex was essentially the same as that for [Ga(*l*-moba)$_3$].

[In(*l*-moba)$_3$]. To a suspension of $InCl_3$·$3H_2O$ (0.13 g) and H(*l*-moba) (0.5 g) in methanol (20 cm^3) was added LiOH·H_2O with stirring. The mixture at once formed a clean solution, and further addition of LiOH·H_2O resulted in the formation of a pale yellow precipitate, which was separated by filtration, washed with water, and crystallized from ethanol as almost colorless microcrystals. The yield was 62%.

[In(*l*-moba-Me)$_3$]. The synthesis for this complex was essentially the same as that for [In(*l*-moba)$_3$].

Analytical results for the complexes are given in Table I.

Measurements. Elemental analyses for carbon and hydrogen were obtained at the Elemental Analysis Service Center of Kyushu Unversity. Metal analyses were made on the basis of metal oxides M_2O_3 obtained as ash in the carbon and hydrogen analysis. ^1H NMR spectra (400 MHz) were recorded in $CDCl_3$ on a JEOL JNM-GX400 spectrometer using tetramethylsilane as the internal standard. CD spectra were recorded in CH_2Cl_2 on a JASCO J-600 spectrophotometer. Electronic spectra were obtained with a Shimadzu MSP-500 spectrometer in the same solvent.

Results and Discussion

Each of the *fac* and *mer* isomers of [M(*l*-moba)$_3$] and [M(*l*-moba-Me)$_3$] consists of diastereomers, Δ(l) and Λ(l), with respect to the central ion and the chirality of the menthyl group. Previously, we have shown that ^1H NMR technique is very useful

Table I. Analytical Data[a]

	% found			% calcd		
	C	H	M	C	H	M
[Sc(*l*-moba)$_3$]	72.74	8.14	4.32	72.92	7.96	4.55
[Sc(*l*-moba-Me)$_3$]	73.42	8.27	4.10	73.44	8.22	4.36
[Y(*l*-moba)$_3$]0.5·H_2O	68.91	7.69	8.96	69.22	7.65	8.54
[Y(*l*-moba-Me)$_3$]0.5·H_2O	70.17	7.97	8.68	69.85	7.91	8.21
[La(*l*-moba)$_3$]0.5·H_2O	65.89	7.52	12.40	66.04	7.30	12.73
[La(*l*-moba-Me)$_3$]0.5·H_2O	66.52	7.83	11.69	66.77	7.56	12.26
[Al(*l*-moba)$_3$]	73.97	8.37	2.51	74.28	8.10	2.78
[Al(*l*-moba-Me)$_3$]	74.47	8.65	2.21	74.75	8.36	2.67
[Ga(*l*-moba)$_3$]	70.92	8.03	6.98	71.14	7.76	6.88
[Ga(*l*-moba-Me)$_3$]	71.40	8.25	7.06	71.72	8.02	6.61
[In(*l*-moba)$_3$]	67.70	7.69	10.53	68.11	7.43	10.85
[In(*l*-moba-Me)$_3$]	68.52	7.88	10.07	68.78	7.70	10.44

[a] *l*-moba = $C_{20}H_{26}O_3$; *l*-moba-Me = $C_{21}H_{28}O_3$.

to estimate the abundances of the geometrical isomers *fac*/*mer* for 1/3 cobalt(III) complexes with unsymmetrical 1,3-diketones.[7] This method depends on the criteria that when the geometrical isomers are obtained in the statistical ratio (*fac*/*mer* = 1/3), the NMR spectrum shows four methine signals with the same intensity (one from the *fac* isomer and three from the *mer* isomer) and that when interligand noncovalent interactions operate within a complex molecule to afford the *fac* isomer predominantly, only one methine signal (or one intense and three less intense methine signals) is observed in the NMR spectrum. This NMR technique can be applicable to configurational analysis of complexes if the isomerization reaction is very slow relative to the NMR time scale.

The Sc, Y, La, and In complexes showed one signal in the methine proton region (6.3–6.8 ppm). This is probably due to fast *fac*–*mer* isomerization[22] but not very high stereoselectivity, affording only the *fac* isomer. When the free ligand was added, the methine signal of the noncoordinated ligand appeared at 6.559 ppm, irrespective of the complex used or the concentration of the free ligand added. The result indicates that isomerization by an intermolecular mechanism is very slow, as generally demonstrated for complexes of those ions.[22] The fast *fac*–*mer* isomerization must be achieved by an intramolecular mechanism such as a rhombic twisting mechanism[23] or Bailar's twist mechanism.[24]

In our preliminary investigations the Al and Ga complexes each showed a ^1H NMR spectrum comprising one main signal and three less intense signals in the methine proton region (cf. spectrum of Figure 3). First, this appeared to be an indication of a predominant formation of a *fac* isomer over a *mer* isomer. Later, we noticed that the NMR spectra of the Al complexes were changeable after dissolution, and on the basis of the time course of the spectra, we arrived at the conclusion that all four diastereomers were equilibrated in solution.

The NMR spectra of [Al(*l*-moba-Me)$_3$] (methine proton region) at various times after dissolution are given in Figure 3. The time dependence of the NMR spectra clearly indicates that the isolated sample of [Al(*l*-moba-Me)$_3$] has a diastereomer distribution different from that in solution and that the equilibration is achieved only slowly in solution. Spectrum a, determined soon after dissolution, comprises three main signals and three very weak signals that are numbered 1–6 from low field. Apparently, signals 1, 3, and 6 increase with time while signal 2 decreases with time. It is not apparent from the spectra whether signals 4 and 5 are changing or not. In order to make proper assignments of the methine signals, their peak heights relative to that of tetramethylsilane added as an internal standard were plotted against time (Figure 4). As is seen in Figure 4, peaks 1, 3, and 6 show a similar time of increase, and they can be assigned to one of the *mer* isomers (*mer*-A). Signals 2, 4, and 5 are also similar, on the whole, in the time of decrease, and they can be assigned to the

(22) Fay, R. C.; Piper, T. S. *J. Am. Chem. Soc.* **1963**, *85*, 500; *Inorg. Chem.* **1964**, *3*, 348.
(23) Ray, P. C.; Dutt, N. K. *J. Indian Chem. Soc.* **1941**, *18*, 289; **1943**, *20*, 81.
(24) Bailar, J. C., Jr. *J. Inorg. Nucl. Chem.* **1958**, *8*, 165.

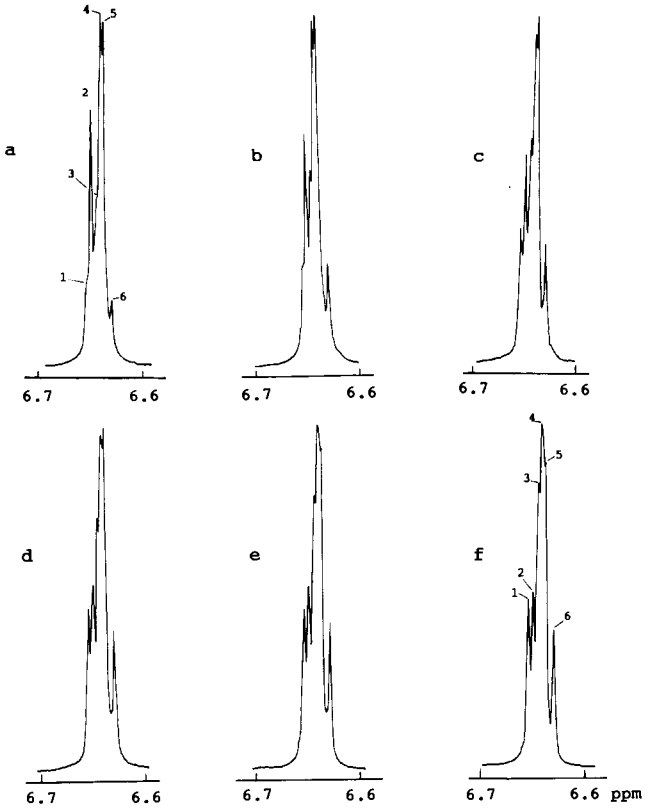

Figure 3. ^{1}H NMR spectra (methine proton region) of [Al(*l*-moba-Me)$_3$] at various times after dissolution (in $CDCl_3$, 400 MHz): a, 5 min; b, 10 min; c, 25 min; d, 45 min; e, 80 min; f, 120 min.

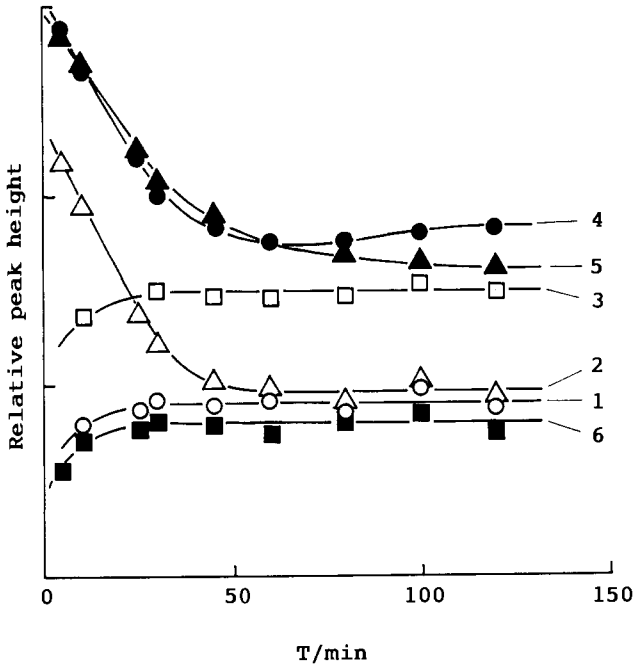

Figure 4. Time course of relative peak heights of the methine protons for [Al(*l*-moba-Me)$_3$]. Peak heights are represented relative to that of TMS added as the internal standard.

other form (*mer*-B) of the *mer* isomers. However, signals 4 and 5 are apparently more intense than signal 2 throughout spectra a–f and signal 4 tends to increase at the final stage (spectra e–f). Presumably, this is due to the fact that there are other signals attributable to the *fac* isomers around 6.64 ppm and the *fac* isomers are also equilibrated in solution.

On the basis of the above assignments and from the evaluations of the peak areas of the methine signals, we estimated the relative abundances of the *mer*-A, *mer*-B, and *fac* (*fac*-Δ and *fac*-Λ) isomers at 1/6/7 soon after dissolution (spectrum a) and at 1/1/4 when the equilibrium was reached (spectrum f). The time course of the NMR spectra for the Ga complexes was not studied in detail because the equilibration was so fast as to be completed within a few minutes. The assignments and the relative abundances of the diastereomers for the Al and Ga complexes are given in Table II. It is to be noticed that the *fac*/*mer* ratio ((*fac*-Δ + *fac*-Λ)/(*mer*-Δ + *mer*-Λ)) exceeds the statistical value (1/3) for all the Al and Ga complexes. This fact is a good indication of the operation of noncovalent interligand interactions within the complex molecule. In general, the *fac*/*mer* ratio increases on going from the Al to the Ga complex in each ligand system or going from the *l*-moba to *l*-moba-Me complex in each metal system.

In the predominating *fac* isomer one of the diastereomers (Δ(l) and Λ(l)) must predominate over the other, as suggested from the NMR spectra of the Al and Ga complexes. For the present complexes the shifts of the equilibrium were inspected by use of circular dichroism induced at the π–π^* transition of the 1,3-diketonate ion.

Table II. NMR Spectral Data

complex	chemical shift, δ/ppm			assgnt[a]	rel abundance
[Sc(*l*-moba)$_3$]	6.757				
[Sc(*l*-moba-Me)$_3$]	6.716				
[Y(*l*-moba)$_3$]	6.406				
[Y(*l*-moba-Me)$_3$	6.372				
[La(*l*-moba)$_3$]	6.336				
[La(*l*-moba-Me)$_3$]	6.332				
[Al(*l*-moba)$_3$]	6.699	6.689	6.675	*mer*-A	1
	6.689	6.681	6.678	*mer*-B	1
		6.676		*fac*	1.5
[Al(*l*-moba-Me)$_3$]	6.654	6.644	6.630	*mer*-A	1
	6.649	6.642	6.638	*mer*-B	1
		6.642		*fac*	4
[Ga(*l*-moba)$_3$]	6.651		6.623	*mer*-A	1
	6.643		6.635	*mer*-B	1
		6.642		*fac*	4
[Ga(*l*-moba-Me)$_3$]	6.651		6.570	*mer*-A	1
	6.609	6.597	6.591	*mer*-B	1
		6.602		*fac*	6.6
[In(*l*-moba)$_3$]		6.617			
[In(*l*-moba-Me)$_3$]		6.580			

[a] *fac*: *fac*-Δ + *fac*-Λ.

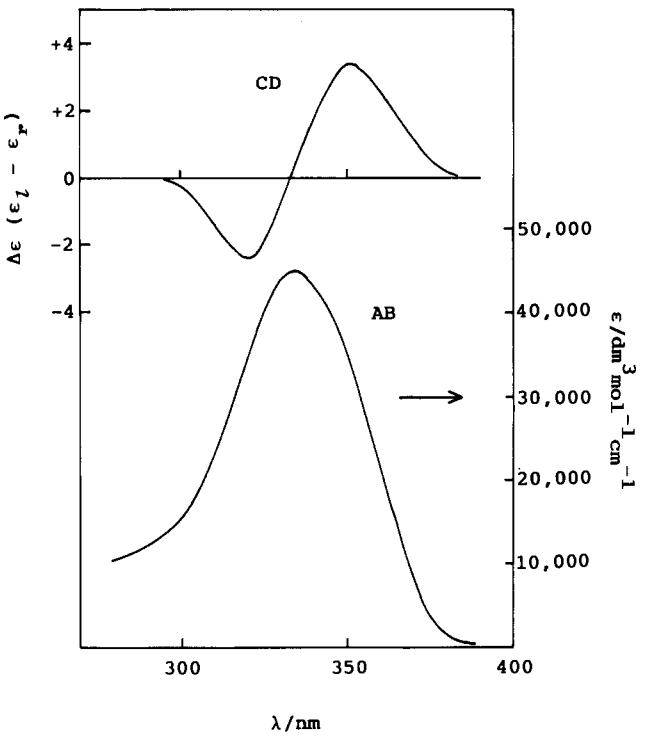

Figure 5. Electronic absorption and circular dichroism spectra of [Sc(*l*-moba-Me)$_3$] in CH_2Cl_2.

Table III. Absorption (AB) and CD Spectral Data

	CD $\Delta\epsilon$ (λ/nm)		AB λ_{max} (ϵ)
[Sc(*l*-moba)$_3$]	−2.4 (321)	+3.4 (351)	334 (44 900)
[Sc(*l*-moba-Me)$_3$]	−4.2 (322)	+5.3 (353)	335 (45 200)
[Y(*l*-moba)$_3$]	−6.4 (318)	+7.2 (349)	334 (43 400)
[Y(*l*-moba-Me)$_3$]	−8.3 (326)	+9.5 (335)	335 (43 500)
[La(*l*-moba)$_3$]	−7.6 (320)	+8.6 (355)	336 (41 600)
[La(*l*-moba-Me)$_3$]	−11.1 (322)	+11.1 (356)	336 (41 900)
[Al(*l*-moba)$_3$]	−0.38 (316)	+0.45 (346)	326 (71 800)
[Al(*l*-moba-Me)$_3$]	−1.7 (317)	+1.7 (347)	326 (70 900)
[Ga(*l*-moba)$_3$]	−1.2 (316)	+1.7 (343)	324 (63 900)
[Ga(*l*-moba-Me)$_3$]	−3.0 (318)	+3.5 (348)	325 (64 500)
[In(*l*-moba)$_3$]	−4.2 (314)	+5.5 (343)	322 (47 800)
[In(*l*-moba-Me)$_3$]	−5.8 (318)	+6.7 (347)	323 (47 600)

Absorption and CD spectra of [Sc(*l*-moba)$_3$] in dichloromethane are shown in Figure 5. The intense absorption band in the near-UV region is assigned to the π–π^* transition band of the diketonate ion.[20] This absorption consists of two components, a shoulder with a moderate intensity near 350 nm and a main peak at 335 nm. Two CD bands corresponding to the components were observed at 353 nm (positive) and att 322 nm (negative). Free ligands showed no CD at the π–π^* transition, indicating that the vicinal effect of the *l*-menthyl group on the π–π^* transition is very small. Therefore, the Cotton effect observed at the ligand π–π^* transition comes from the dissymmetry or asymmetry induced at the central ion. Similarly, the other complexes also showed two CD bands at the ligand π–π^* band. The CD spectral results (after equilibration) are given in Table III along with the absorption spectral data.

It is seen that the CD pattern observed at the ligand π–π^* transition is the same for all the complexes: + and − signs from longer wavelength. Hence, we presume the configuration of the diastereomer existing in the largest excess in solution to be the same for all the complexes. This presumption makes sense if the stereoselectivity of the complexes is mainly caused by the noncovalent interaction as depicted in Figure 1. From detailed studies on electronic absorption and CD spectra of (−)-[Si(acac)$_3$]$^+$ (which has the CD pattern of − and + signs from longer wavelength), Larsen et al.[20] determined its absolute configuration as Δ. In view of their assignment, the configuration of the predominant diastereomer of [M(*l*-moba)$_3$] and [M(*l*-moba-Me)$_3$] in the equilibrated solution is concluded to be *fac*-Λ. This differs from our previous assignment (*fac*-Δ) to the cobalt(III) and chromium(III) complexes.[2,3,5]

In order to make more explicit assignments of configurations, we studied the time course of CD spectra of the Al complexes. The CD spectra of [Al(*l*-moba-Me)$_3$] at various times after dissolution are given in Figure 6. The spectrum soon after dissolution (spectrum a) shows very intense CD bands with the negative and positive signs from longer wavelength, indicating the preferred absolute configuration to be Δ, which is indeed the configuration assigned previously to the isolated samples of the cobalt(III) and chromium(III) complexes.[2,3,5] The CD bands of [Al(*l*-moba-Me)$_3$] were weakened with time, and after 2 h the spectral pattern changed to that of the Λ configuration. Evidently, the diastereomeric distribution in solution changes with time, with the *fac*-Δ form in the largest excess at the early stage and the *fac*-Λ form in the largest excess after equilibration. Further, together with the NMR spectral results discussed above, the configuration of *mer*-A is assigned to Λ and the configuration of *mer*-B to Δ.

The above results suggest that the *fac*-Δ form is favored for crystal packing, and thence this form has been crystallized from an equilibrated solution of the diastereomers. In order to gain evidence for this presumption, we recovered [Al(*l*-moba-Me)$_3$] from its equilibrated dichloromethane solution by different methods and examined the CD spectra of the recovered samples. The sample obtained by very slow evaporation of the solvent formed crystals, and its dichloromethane solution showed a CD spectrum very similar to spectrum a in Figure 3. On the other hand, the sample obtained by a quick evaporation of the solvent at room temperature formed an amorphous precipitate and showed

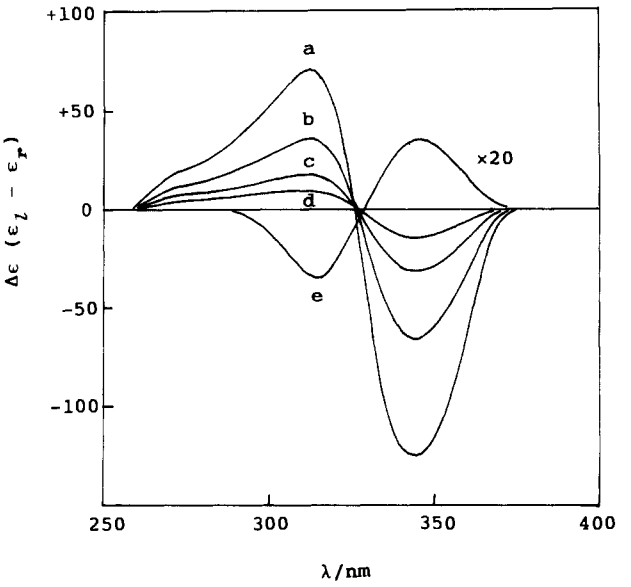

Figure 6. Circular dichroism spectra of [Al(*l*-moba-Me)$_3$] at various times after dissolution: a, 5 min; b, 15 min; c, 25 min; d, 35 min; e, 120 min.

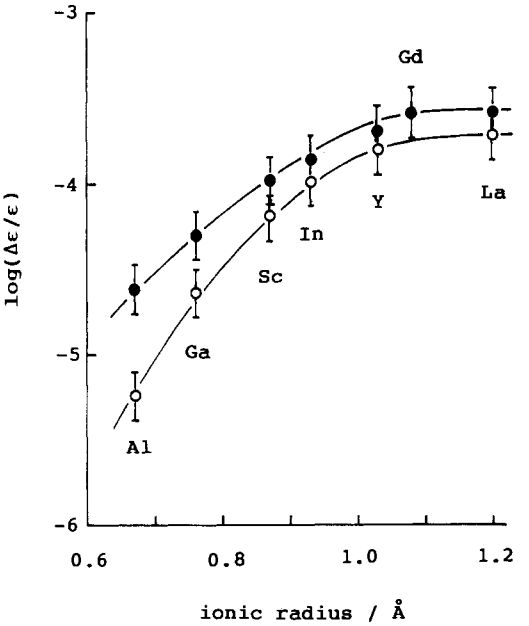

Figure 7. Relation between logarithmic asymmetric factors (log ($\Delta\epsilon/\epsilon$)) and ionic radii for [M(*l*-moba)$_3$] (○) and [M(*l*-moba-Me)$_3$] (●).

a spectrum similar to spectrum f in Figure 3. It is evident that the *fac*-Δ form is more favored in crystals while the *fac*-Λ form is more stable in solution. In our reinvestigations on [Co(*l*-moba-Me)$_3$] and [Cr(*l*-moba-Me)$_3$], the reaction mixture[25] showed practically no CD at the first d–d band region but the *fac*-Δ form was indeed isolated in a crystalline form in each case. *fac*-Δ-[Co(*l*-moba-Me)$_3$] dissolved in dichloromethane showed little CD spectral change for 5 weeks. A similar high stability toward racemization was found for [Co(acac)$_3$].[26,27] *fac*-Δ-[Cr(*l*-moba-Me)$_3$] in dichloromethane showed a slight decrease in the CD intensity after 5 weeks, indicating very slow racemization.

(25) The cobalt complex was synthesized by air oxidation of an ethanolic solution of [Co(*l*-moba-Me)$_2$(H$_2$O)$_2$] and H(*l*-moba-Me) (excess). The chromium complex was synthesized by the reaction of $CrCl_3 \cdot 6H_2O$ and H(*l*-moba-Me) (excess) in the presence of triethylamine and a small amount of charcoal.

(26) Collman, J. P.; Blair, R. P.; Slade, L.; Marshall, R. L. *Chem. Ind. (London)* **1962**, 141.
(27) Collman, J. P.; Blair, R. P.; Marshall, R. L.; Slade, L. *Inorg. Chem.* **1963**, *2*, 576.

The racemization was expected to be much accelerated at elevated temperature,[22] but the chromium complex was found to decompose in hot solution. Hence, we could not clearly demonstrate if the equilibrium among the diastereomers also shifts in favor of *fac*-Λ in these cobalt(III) and chromium(III) complexes. However, the present study strongly suggests that noncovalent interligand interactions undoubtedly operate within a complex molecule, though its true depiction is not the right-handed (Figure 2) but the left-handed three-bladed propeller. In view of the above facts, we must retract a part of our previous conclusions on the cobalt(III) and chromium(III) complexes.[2,3,5]

It is seen from Table III that the CD induced at the ligand π–π^* transition is more intense in [M(*l*-moba-Me)$_3$] than in [M(*l*-moba)$_3$]. Hence, a higher stereoselectivity occurs in the *l*-moba-Me complexes, in agreement with the NMR spectral results for the Al and Ga complexes. This is probably due to a more efficient interaction in the *l*-menthyl/*p*-tolyl pair than in the *l*-menthyl/phenyl pair probably because of the increased π-electron density in the *p*-tolyl ring.[5,6] Table III further shows that the CD intensity increases on going from the Al to the In complex and from the Sc to the La complex in each ligand series. These facts imply that the CD intensity tends to increase when the central metal ion becomes larger, and this trend is more prominent when we adopt the asymmetry factor ($\Delta\epsilon/\epsilon$) instead of $\Delta\epsilon$, where the average is taken for the absolute values of two CD bands. When the $\Delta\epsilon/\epsilon$ values observed are plotted against the ionic radii (Shannon–Prewitt ionic radii[28]) of the metal ions, a good correlation is found between them, as shown in Figure 7. In this figure the data for [Gd(*l*-moba-Me)$_3$] determined in this study[29] are also included. The present result implies that efficient interligand *l*-menthyl/aryl interaction in [M(*l*-moba)$_3$] and [M(*l*-moba-Me)$_3$] becomes possible when the interacting groups can adopt a mutual orientation favorable for the interaction, and the ideal spatial matching of the interacting groups is attained when the central metal ion is considerably large ($r > 1.0$ Å). The above finding adds strong support to the noncovalent interligand interaction operating within complex molecules in the form of a left-handed three-bladed propeller.

This work was supported by Grant-in-Aid for Scientific Research No. 62430011 from the Ministry of Education of Japan. We are grateful to K. Ogi for NMR measurements and to H. Sakiyama for help in CD measurements.

(28) Shannon, R. D.; Prewitt, C. T. *Acta Crystallogr.* **1969**, *B25*, 925.
(29) Spectral data are as follows: AB, 336 nm (ϵ 40 500); CD, 351 nm ($\Delta\epsilon$ +12.3) and 318 nm ($\Delta\epsilon$ −8.8).

Contribution from the Department of Chemistry, The University of Texas, Austin, Texas 78712

Electrochemistry in Liquid Sulfur Dioxide. 8. Oxidation of Iron, Ruthenium, and Osmium Bipyridine Complexes at Ultramicroelectrodes at Very Positive Potentials

Edwin Garcia, Juhyoun Kwak, and Allen J. Bard*

Received April 12, 1988

The anodic potential range of liquid SO_2 for use in electrochemical studies was extended to about +4.7 V vs SCE by employing a new purification method and using tetra-*n*-butylammonium hexafluoroarsenate [(TBA)AsF_6] as supporting electrolyte. The anodic solvent limit occurs at potentials 0.7 V more positive than in previous studies and is attributed to supporting electrolyte oxidation. The electrochemistry of M(bpy)$_3^{2+}$ complexes (M = Fe, Ru, and Os) at −70 °C was studied by cyclic voltammetry at an ultramicroelectrode (25 μm diameter, Pt) with scan rates up to 10 kV/s. Fe and Ru oxidation waves to the 3+ form (metal-centered oxidation), and 4+, 5+, and 6+ species (bpy-centered oxidations) are observed. While the 4+ forms were stable, the 5+ and 6+ species decomposed, presumably by reaction with solvent or supporting electrolyte. For M = Os, waves for oxidation of stable, metal-center 3+ and 4+ species are observed. A third wave, to an unstable 5+ species, represented as $Os^{IV}(bpy^{\cdot+})(bpy)_2$, is also seen. Standard potentials for these waves and rate constants for the decomposition of the 5+ and 6+ species are estimated. The order of stabilities of the highly oxidized forms is Fe(5+) ~ Ru(5+) > Os(6+) > Ru(6+) > Fe(6+).

Introduction

To generate highly oxidizing species electrochemically and to study their properties requires a solvent/supporting electrolyte system that will not oxidize at an electrode until very positive potentials and will not react rapidly with the electrogenerated species. Thus the introduction of acetonitrile and other aprotic solvents allowed the study of radical cations and difficultly oxidized organic and inorganic species. Liquid SO_2 has been especially useful in such studies,[1-8] and by careful purification and the use of tetra-*n*-butylammonium fluoroborate [(TBA)BF_4] as supporting electrolyte, an anodic range to +4 V vs SCE was reported. Previous studies from this laboratory described the electrochemical oxidation of the complexes M(bpy)$_3^{2+}$ (where M = Ru, Fe, and Os and bpy is 2,2′-bipyridine),[1] in SO_2 solutions containing (TBA)BF_4 or (TBA)PF_6 as supporting electrolytes. In these studies, oxidations of the Ru complex to the 4+ form near the oxidation background limit was observed. For the Fe complex, oxidation to both the 4+ and 5+ states was reported. Although reversibility of the $FeL_3^{3+/4+}$ (L = bpy) couple was found with cyclic voltammetry (CV) higher scan rates (≥10 V/s), reactions of the FeL_3^{5+} and the RuL_3^{4+} with a solution component to regenerate the lower oxidized form (in a catalytic reaction mechanism) occurred and reversal (reduction) waves for these species were not seen. With OsL_3^{2+} as starting material, both the 3+ and the 4+ species were stable; more highly oxidized species were not found.

We describe here studies with liquid SO_2 prepared by an improved purification procedure and with (TBA)AsF_6 as supporting electrolyte to produce a significantly extended anodic solvent/electrolyte limit. Moreover, by using an ultramicroelectrode,[9-17]

(1) (a) Gaudiello, J. G.; Sharp, P. R.; Bard, A. J. *J. Am. Chem. Soc.* **1982**, *104*, 6373. (b) Gaudiello, J. G.; Bradley, P. G.; Norton, K. A.; Woodruff, W. H.; Bard, A. J. *Inorg. Chem.* **1984**, *23*, 3.
(2) Tinker, L. A.; Bard, A. J. *J. Am. Chem. Soc.* **1979**, *101*, 2316.
(3) Tinker, L. A.; Bard, A. J. *J. Electroanal. Chem. Interfacial Electrochem.* **1982**, *133*, 275.
(4) Sharp, P. R.; Bard, A. J. *Inorg. Chem.* **1983**, *22*, 2689.
(5) Sharp, P. R.; Bard, A. J. *Inorg. Chem.* **1983**, *22*, 3462.
(6) Anson, F. C.; Collins, J. T.; Gipson, S. L.; Keech, J. T.; Kraft, T. E. *Inorg. Chem.* **1982**, *26*, 1157.
(7) Miller, L. L.; Mayeda, E. A. *J. Am. Chem. Soc.* **1970**, *92*, 5818.
(8) Diethrich, M.; Mortensen, J.; Heinze, J. *Angew. Chem., Int. Ed. Engl.* **1985**, *24*, 508 and references therein.
(9) (a) Wightman, R. M. In *Electroanalytical Chemistry*; Bard, A. J., Ed.; Marcel Dekker: New York, 1988; Vol. 15, in press. (b) Fleishmann, M.; Pons, S.; Rolison, D.; Schmidt, P. P. *Ultramicroelectrodes*; Datatech Science: Morganton, NC, 1987.
(10) Howell, J. O.; Wightman, R. M. *Anal. Chem.* **1984**, *56*, 524.
(11) Howell, J. O.; Wightman, R. M. *J. Phys. Chem.* **1984**, *88*, 3915.

0020-1669/88/1327-4377$01.50/0 © 1988 American Chemical Society